

Chapter 5

The Active-Matrix Pixel Structure

Application in Field Emission Display

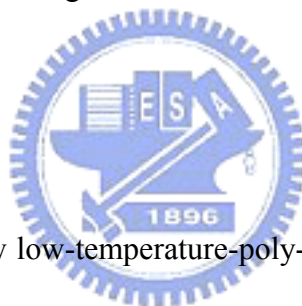
5.1 Introduction

Nowadays, Flat Panel Displays (FPDs) have been widely applied in monitors, televisions, portable displays and so on in the recent years. Dozens of researches and technologists were invested into the business. The liquid crystal displays are the most popular technology due to its light weight, high reliability, and matured thin film process; however, it still suffers from low contrast, low brightness and long response time for video pictures. On the other way, field emission displays (FEDs) attracted much attention since 1990s and are one of the promising candidates for the next generation display due to its high brightness, low fabrication cost, short response time and wide viewing angle. Spindt-type FEDs have been fabricated and demonstrated [18], however the operation voltage is too high and the tips easy to deactivation. The active matrix (AM) driving scheme was proposed to solve these issues before in the spindt-type FEDs. The high blocking voltage device such as the lateral diffused MOSFET must be used to prevent the breakdown from the high operation voltage of FEDs. However, the fabrication cost was too high to integrate the MOSFET process and FED process. The carbon-nanotube (CNT) [19] in recent years took the place of spindt tips because of its low work function which leads to low turn-on electric field and low operation voltage. Even more, the large area display of CNT-FEDs can be realized by a very low cost process, such as the screen printing technology. But, unfortunately, non-uniform for brightness and turn-on voltage are still the main issues of CNT-FEDs. To solve these problems, we try to propose thin film transistors (TFTs)

as the active devices to control the emission current of CNTs.

In this chapter, low-temperature-poly-silicon (LTPS) TFTs were adopted as the switching and driving device of diode-CNT because the traditional amorphous-silicon TFTs could not endure the relative high-temperature sealing process of CNT-FEDs [113]. The active-matrix addressing schemes proposed before were almost the impulse type display [65-67]. Here we proposed a hold-type pixel structure. And a long channel structure of driving TFTs were designed and fabricated to withstand high blocking voltage across the drain to source of TFTs when the CNT is turned off. That could improve the stability of active-matrix CNT-FEDs. Moreover, LTPS TFTs have the high capabilities of integration with some driver circuits since its high electrical properties. The scan driver was integrated into this display.

5.2 Experiment



In this chapter, the low low-temperature-poly-silicon TFTs were fabricated in Electrical Research and Service Organization with a standard 7 mask process [114]. And the top gate N-type TFT configuration was adopted here. The substrates used in this experiments were all $370 \times 470 \text{ mm}^2$ OA10 glass from Nippon electrical Glass. The process flow was described as following (See Fig. 5.1). First, a tetraethylorthosilicate (TEOS) oxide of thickness of 300 nm was deposited as a buffer layer by plasma-enhanced chemical vapor deposition (PECVD). Then the active layer of 50 nm thickness a-Si:H was deposited by PECVD and was annealed to crystallize into poly-silicon film by XeCl excimer laser in N_2 atmosphere at room temperature. The lithography and etching process were done to pattern the active region. Then, the source and drain were formed by ion doping. A TEOS oxide layer of thickness 100 nm was then deposited as gate insulator by PECVD at 106.6 Pa and $380 \text{ }^\circ\text{C}$. The gases

He, O₂ and tetraethylorthosilicate (TEOS) were used with the following respective breakdown of gas quantity: 100, 3500, and 175 sccm. Then, a low resistance MoW layer of 300 nm thickness was then sputtered and patterned as the gate electrode. The interlayer of TEOS oxide of 400 nm thickness was deposited and the contact holes were etched. Then, a MoW layer of 300 nm thickness used as the second metal layer was sputtered and patterned. The passivation layer was formed by depositing 700 nm TEOS oxide and the contact holes were then patterned. The indium tin oxide (ITO) of 150 nm thickness was sputtered and patterned as the cathode electrode of CNTs. Finally, the CNTs emitters were then fabricated by screen printing technique and were sintered at temperature of 560 °C [115]. The sintered temperature would strongly affect the CNT-emitter's turn-on electrical field. Usually it could not be lower than 450°C. The cathode plate was done. The whole cathode plate process temperature was controlled under 560°C.

The anode plate contains anode electrode, phosphors and rib spacer. The electrode used here was the transparent ITO of thickness 150 nm. Sometimes the Cr oxide was additional adopted as the black matrix to improve the contrast of the display. The phosphors and the rib spacer were both prepared by screen printing technique. The cathode and the anode were then assembled by the fully vacuum sealing process under 10⁻⁷ torr. The distance between cathode plate and anode plate was varied from 40 μm to 60 μm. It depends on the density and thickness of rib spacers. The detail process was described in [115].

5.3 Result and Discussion

5.3.1 The Proposed Novel Pixel Structure

A new hold-type pixel structure was proposed in this chapter. The schematic

circuit and layout are shown in Fig. 5.2. As shown in this figure, the pixel consists of a diode-CNT, a storage capacitor, a switch TFT and a driving TFT which is used as the driving device to control the emission current of the diode-CNT. When the switch TFT is turned on, the data signal would be stored in storage capacitor (C_{st}) which applied the same voltage to the gate of the driving TFT. Thus the current flowing through the driving TFT can be maintained to be constant in a frame time. By modulating the data signal, the emission current of CNT emitters could be modified. And the brightness of the selected pixels could be controlled. Here, n-type TFTs were chosen instead of p-type in order to stabilize gate to source voltage (V_G), because the source voltage (V_S) could be kept constant during operation, usually at ground. Also, n-type switch TFTs were used to simplify the fabrication process. In this chapter, two basic designs of the driving TFTs are used: one is the conventional single gate structure with the device feature of channel width $8\ \mu\text{m}$ and channel length $16\ \mu\text{m}$, another is the multi gates structure in which the channel of each single gate TFT are in series connection. To prevent the high anode voltage induced TFT breakdown, sometimes, we would add an additional poly-silicon resistor in series with the driving TFT between drain of driving TFT and CNT -emitter's cathode.

A real discrete circuit was made to simulate the active-matrix driving scheme. A single gate LTPS-TFT was series connected with a diode CNT-FED as shown in Fig. 5.3(a). By modulating the gate voltage of the TFT, the current flowing through the diode CNT-FED was modified. The result is shown in Fig. 5.3(b). The anode voltage would be shared by TFT and FED device. From the result, the display scan signal was set to range from 0V to 15V to make sure the switching TFT on and off. The data signal was set to range from -5V to 15V to modulate the emission current. And the anode voltage is set as 160V.

5.3.2 The Characteristics of Carbon Nanotube Field Emission Display

The diode-CNTs prepared by screen printing technique show low turn-on electrical field at about 3 V/um. With the rib layer thickness of 50 um, the turn-on voltage of the diode-CNT is about 150 V. The characteristic of emission current versus CNT voltage was shown in Fig. 5.4(a). The measurement was done in a high vacuum chamber, and the samples were uniformly distributed in four corners of a 4 inch diode CNT-FEDs. Non-uniform turn-on voltages are observed in Fig. 5.4(a) due to different CNT lengths from the same screen printing process. The suppression of this variation is in regard to many conditions, such as the density of CNT emitters, the distribution of CNTs in Ag paste, and the activation of the CNTs. Generally, in the lab, the turn-on voltage of each pixel could be suppressed into ± 20 V around 150 V. Fig. 5.4(b) shows the current-voltage-brightness relation for a diode CNT-FEDs. From this figure, we could see the brightness was nearly proportional to the emission current density and anode voltage. The relation could be expressed as $B \propto I_{CNT} \times V_{anode}$. Here, B is the brightness, I_{CNT} is the emission current and V_{anode} is the anode voltage. Accordingly, we can conclude two important criteria which can be depicted in Fig. 5.5.

5.3.3 The Driving Requirement and Result of Active-Matrix Field Emission Display

Describing the two criteria, first, the TFTs should be designed to possess proper channel length modulation effect or the proper λ value which is measured from the slope of the saturation current. Since the brightness of CNTs is proportion to the product of the emission current and the voltage across CNTs ($I_{CNT} \times V_{anode}$). The

emission current of CNTs was supposed equal to the drain current of the driving TFT. Thus, the uniform brightness can be achieved by choosing the proper λ value to let $I_1(V_{anode}-V_1)=I_2(V_{anode}-V_2)$ in the Fig. 5.5. Second, the TFT devices should be designed to sustain high drain voltage. Because when the driving TFT is turned off, the anode voltage would be shared by the CNT and driving TFT; thus, a large voltage drop will occur at the drain of TFT which may cause drain-side gate oxide breakdown and the pixel may fail. Hence, a special structure for the driving TFT must be designed to fit the two requirements mentioned above.

In this chapter, a TFT with the structure of multi-gate was designed. The top view of the TFT is shown in Fig. 5.6(a). The number of the gates depends on the voltage level that the drain of TFT should be able to sustain. Here, ten gates were adopted to obtain the appropriate electrical characteristic. The $I_{DS}-V_D$ characteristic of the TFTs is shown in Fig. 5.6(b) which shows the required slope of saturation current and high voltage operation stability of 70 V. Also, the current pinching phenomenon [116] which often occurs in the high voltage device is not observed in this TFT. The fabrication process is the same with conventional TFTs, hence no additional masks are needed comparing to other complicated structures [117,118].

Another issue for the application of LTPS-TFT in the active matrix CNT-FEDs was the capability for sustaining the high temperature process of CNT-FED process, which usually under the 560 °C. Fig. 5.7 depicts the LTPS-TFT result before and after 560 °C thermal budget for 30 minutes. The characteristics have been a little twisted. The threshold voltage shift a few volt, and the sub-threshold slop degraded. Nevertheless, the on/off current ratio was still high and enough to modulate the diode CNT-FEDs.

Since LTPS-TFT technology is adopted in the AMCNT panel, some driver circuits can be integrated. In this chapter, the scan driver function is fully integrated

under the CNT high temperature process. The clock swing is controlled to the level below 15 V. Fig. 5.8 shows the result image of the 4-inch QVGA AMCNT panel with resolutions of 320×240. Although the image quality still needs further improvement, it could work successfully.

5.4 Conclusion

In this chapter, the active-matrix pixel structure was proposed and improved for the driving of diode CNT-FEDs. We adopt the high breakdown voltage TFTs to avoid the damage from high anode voltage. The power consumption was supposed to reduce in this hold-type pixel since the emission current of the diode-CNT can be lower compared to pulse-type AMCNT [42] or traditional passive matrix designs. The 4 inch display was successful demonstrated and showing the video images. Scan driver circuits were also integrated into the FED panel with LTPS-TFT technology which is consistent with the technology trend of system on panel. In the future, to improve this technology, the low voltage phosphors are needed, and new pixel structure would be proposed to compensate the requirement of still high anode voltage.

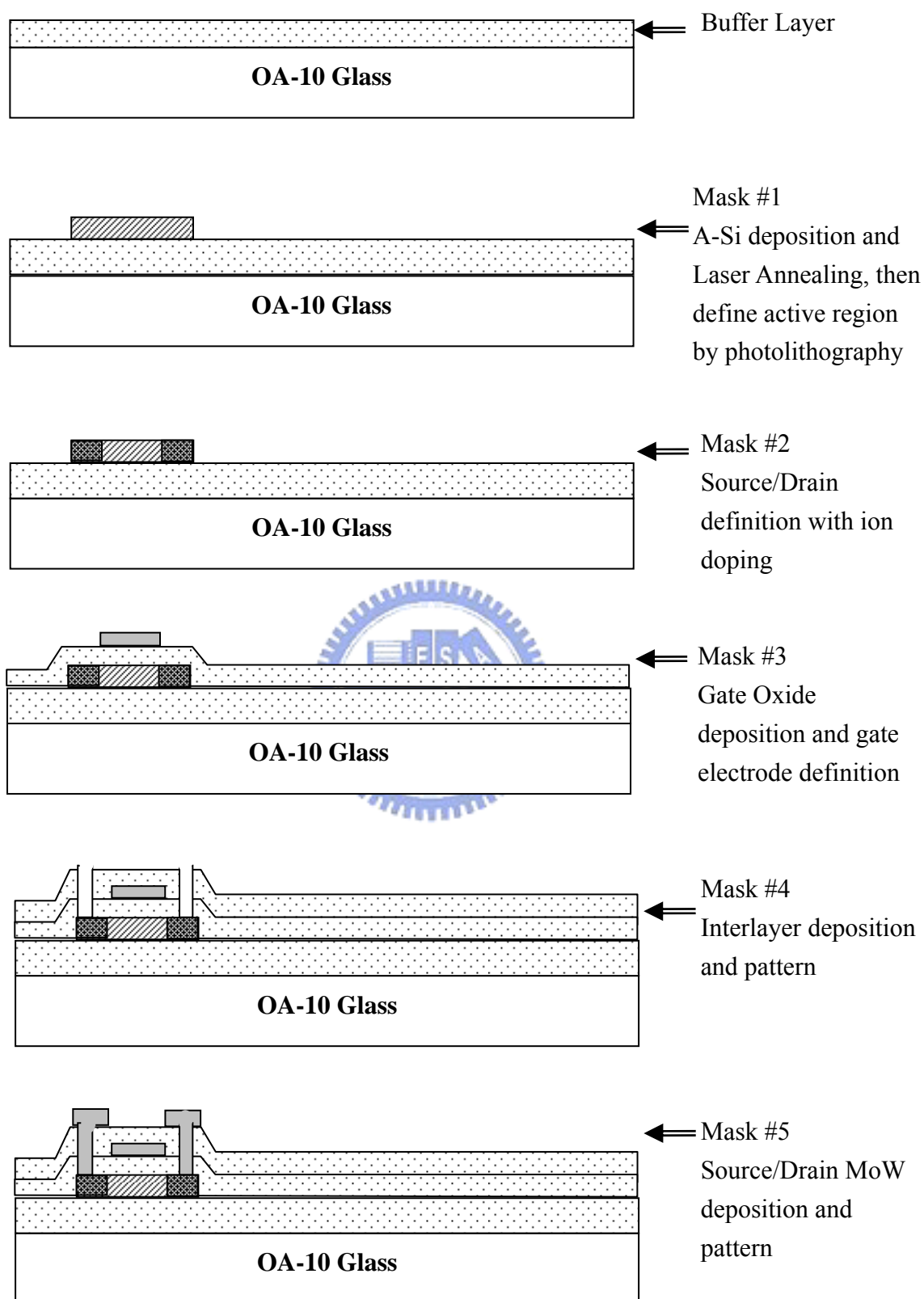


Fig. 5.1 The process flow of the active-matrix CNT-FEDs (to be continued).

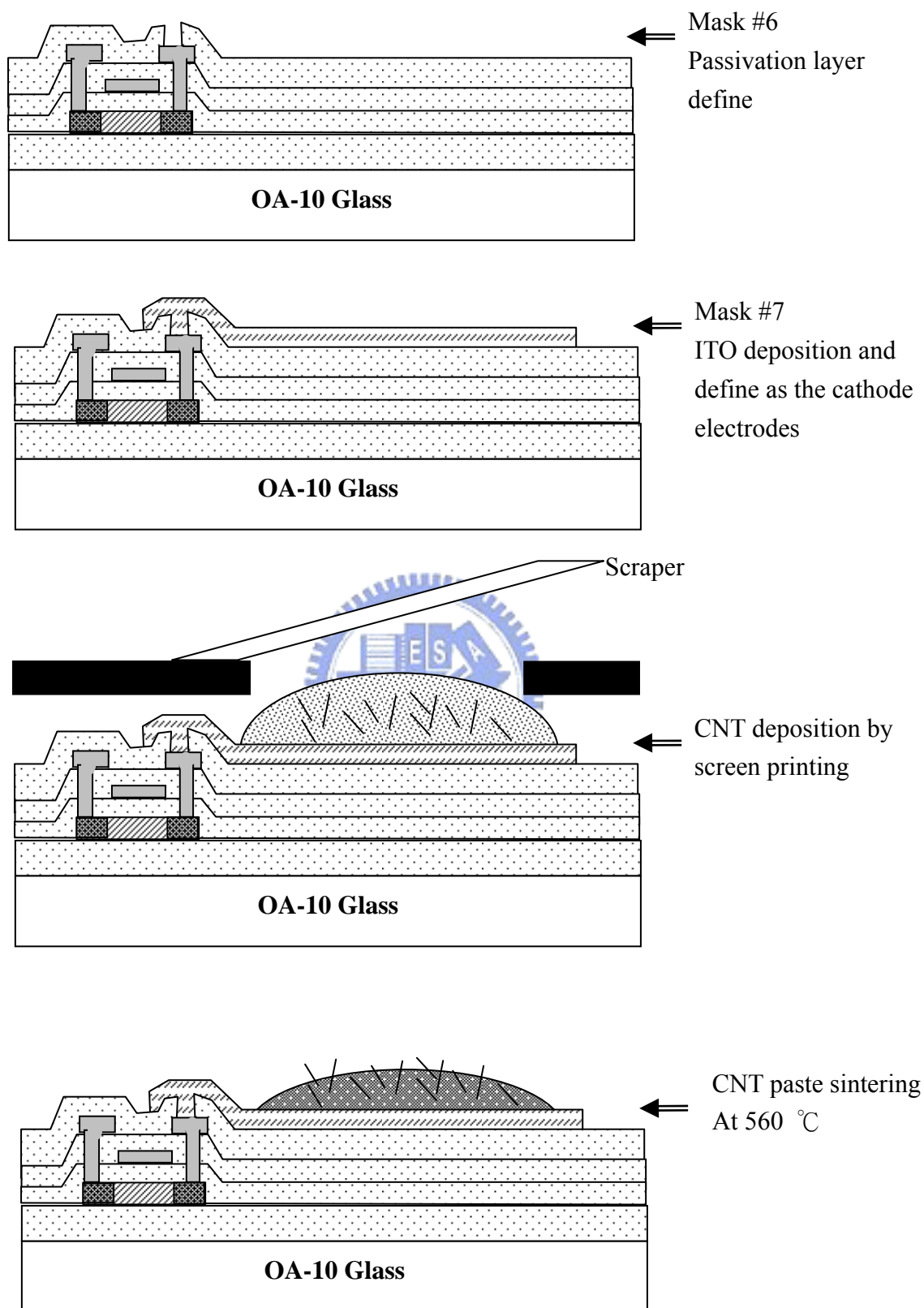


Fig. 5.1 The process flow of the active-matrix CNT-FEDs (to be continued).

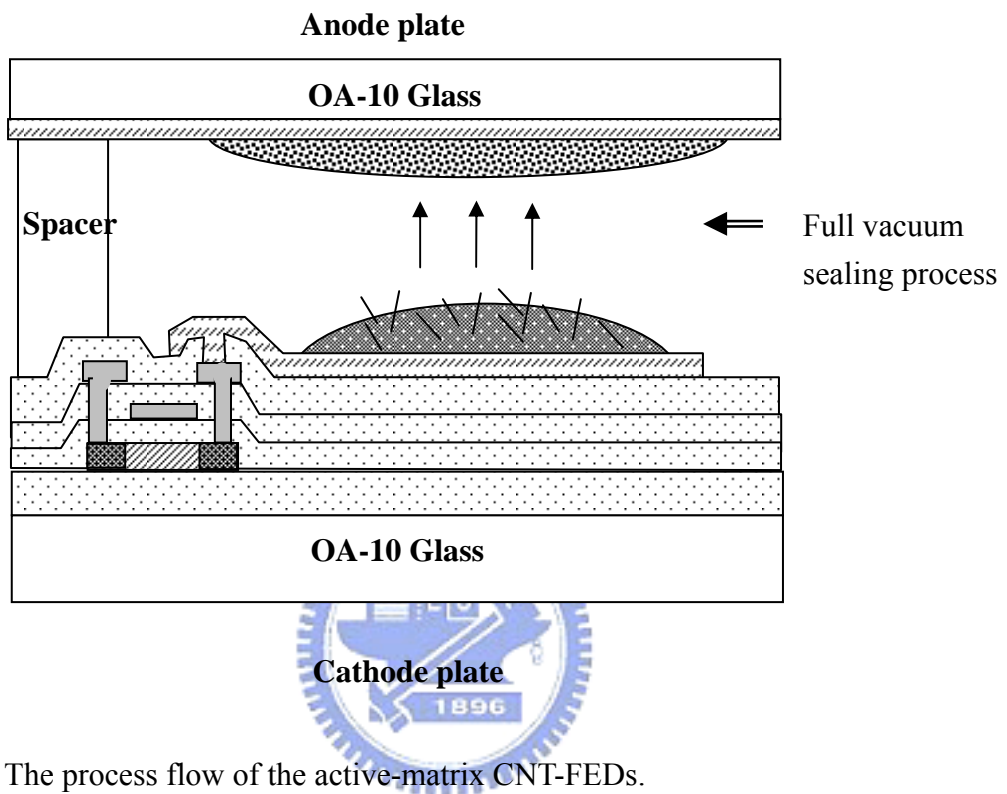
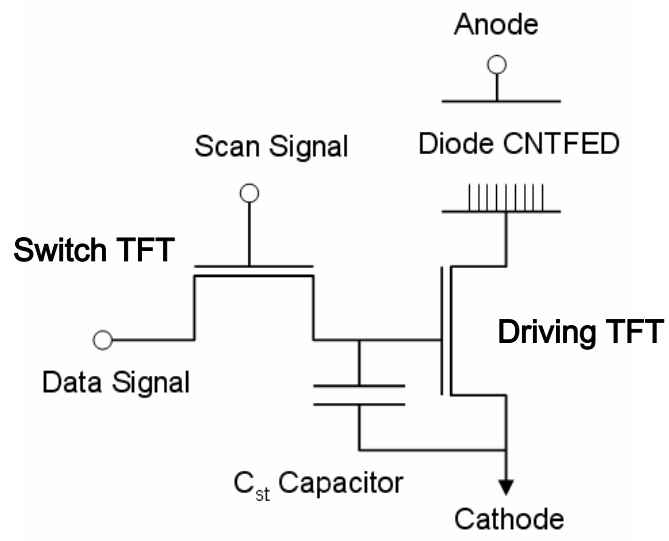
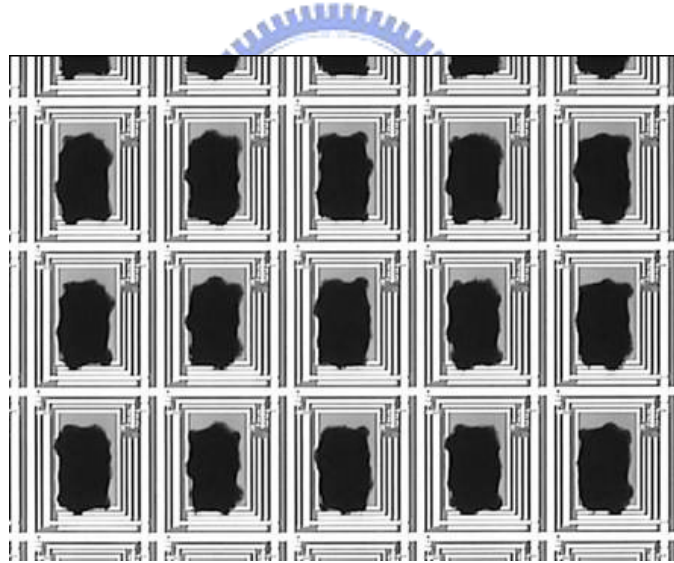


Fig. 5.1 The process flow of the active-matrix CNT-FEDs.



(a)



(b)

Fig. 5.2 (a) Schematic circuit and (b) layout of the novel active-matrix pixel structure.

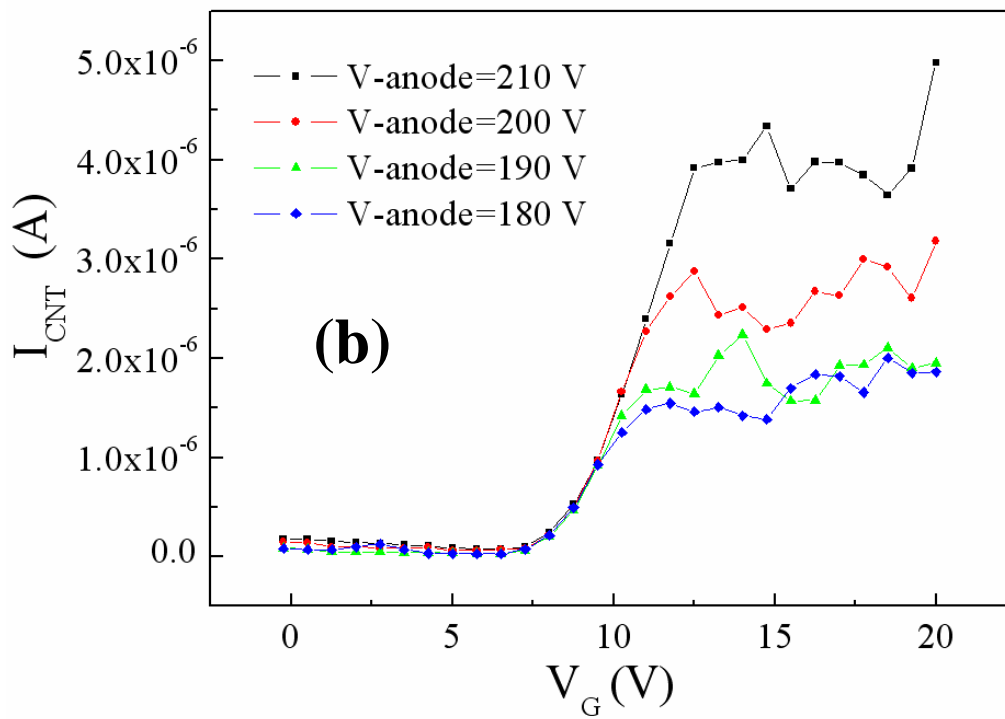
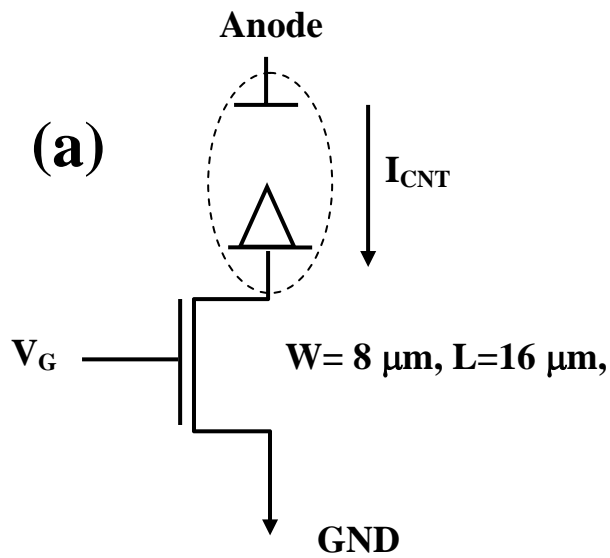


Fig. 5.3 (a) Schematic circuit of the discrete devices including a diode CNT-FED and a n-type TFT with feature size of channel width $8\ \mu\text{m}$ and channel length $16\ \mu\text{m}$, and (b) the transfer characteristics of (a) at different anode voltage.

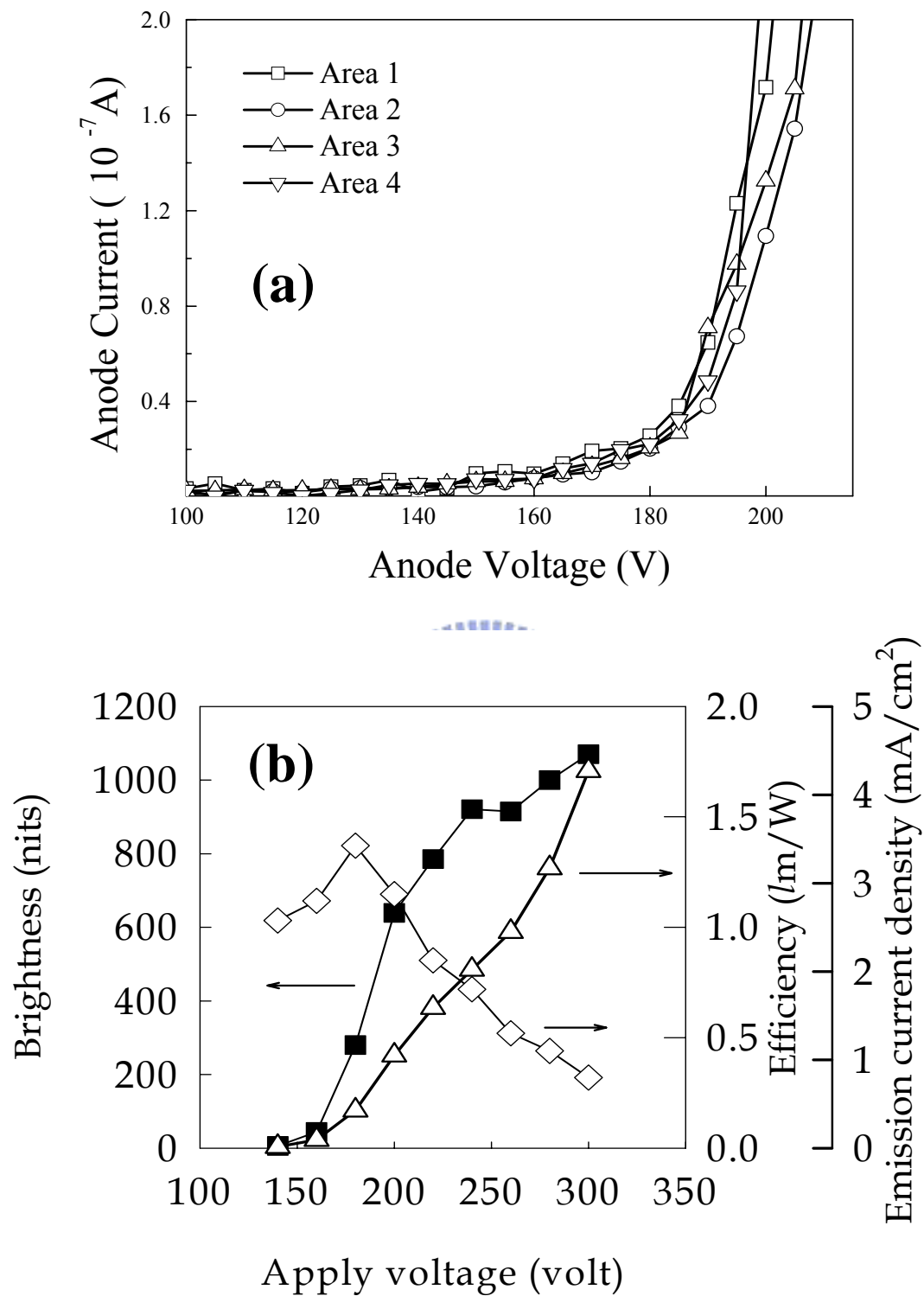


Fig. 5.4 (a) The emission current versus voltage characteristics of diode-CNT FED that were measured from four different areas. (b) The current-voltage-brightness for a diode CNT-FED with 50 μm space distance.

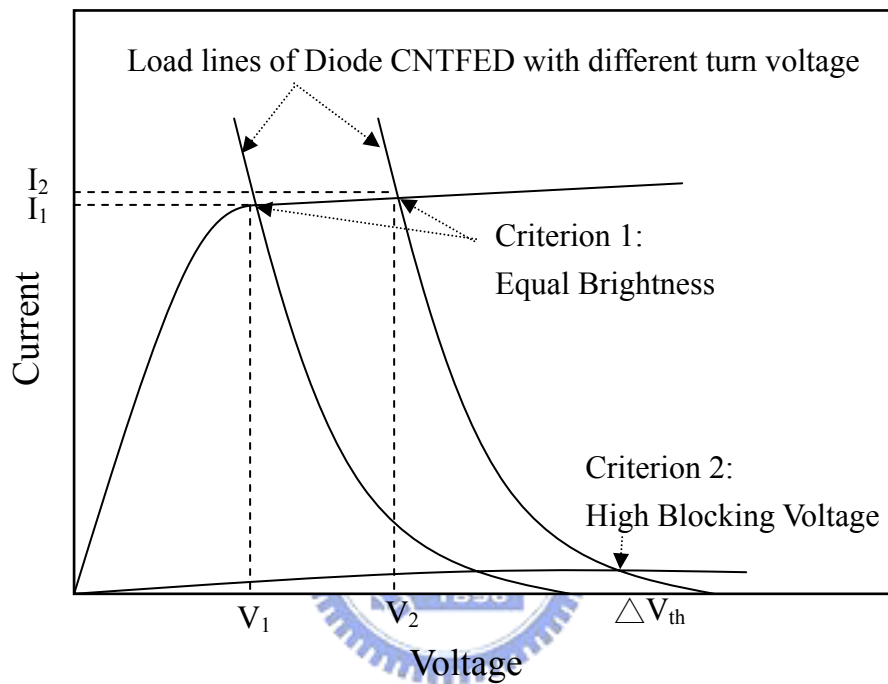
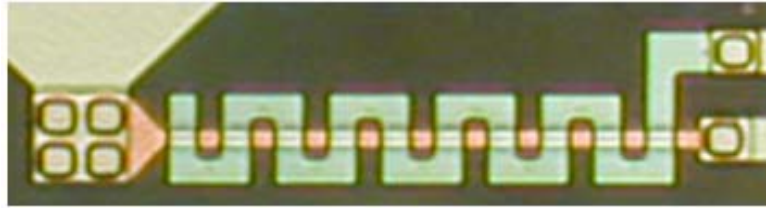
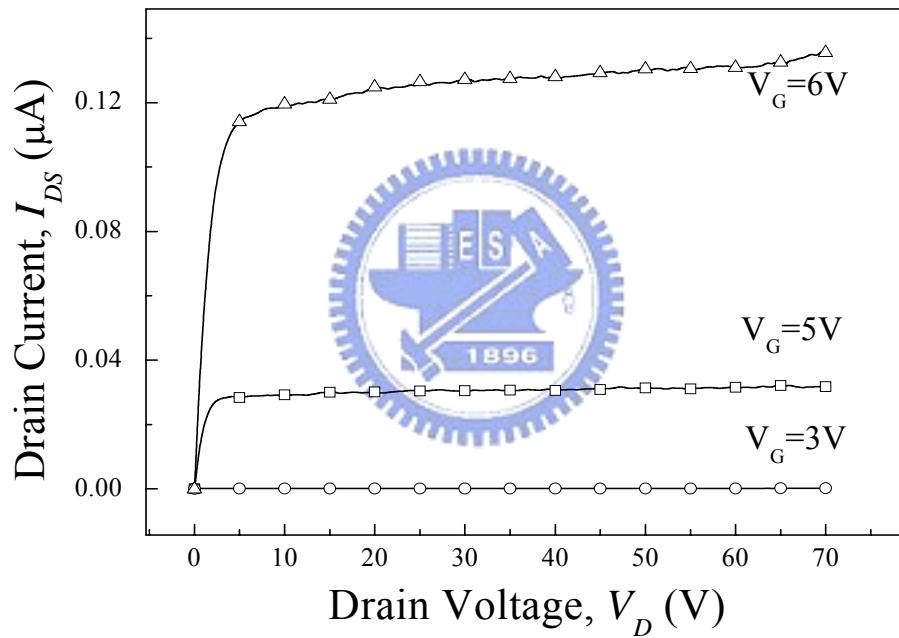


Fig. 5.5 Two criteria of driving TFT that were depicted by TFT's output curves along with CNT's load line.



(a)



(b)

Fig. 5.6 (a) Top view of the multi-gates TFT and (b) the output characteristics of multi-gates TFT.

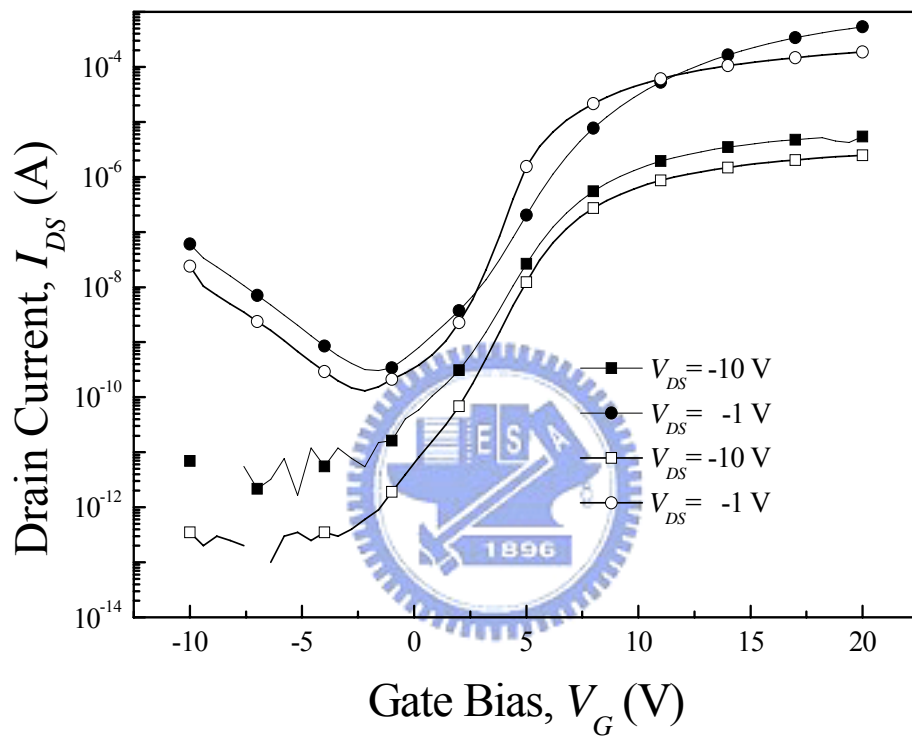


Fig. 5.7 The transfer curves of a single gate LPTS-TFT before and after 560 °C thermal process at V_D of -1 V and -10 V, respectively. The close symbol presents the case after thermal process and the open symbol denotes the origin case. The square symbol was the case at V_D of -1 V, and the circle symbol was the case of V_D of -10 V.

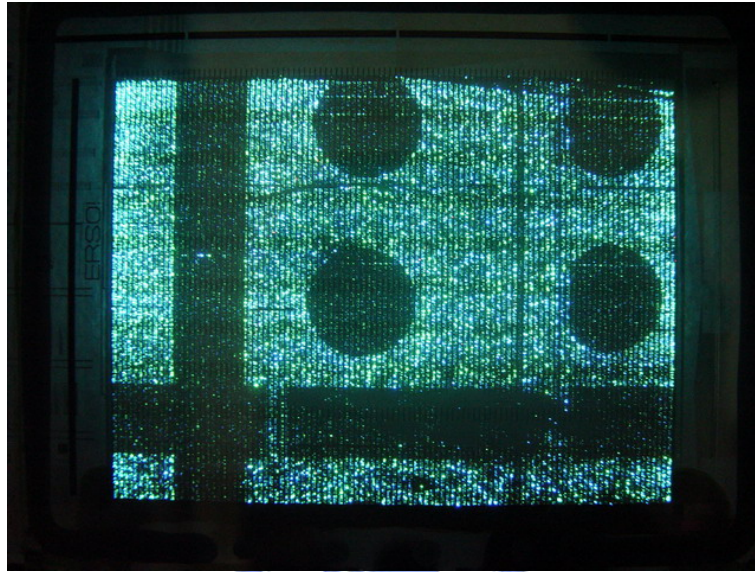


Fig. 5.8 The image of 4 inch active-matrix CNTFED display driven by high voltage TFTs.